

Evolution of Holographic Complexity Near Critical Point

H. Ebrahim^{*},^{1,2} M. Asadi[†],² and M. Ali-Akbari[‡]³

¹*Department of Physics, University of Tehran, North Karegar Ave., Tehran 14395-547, Iran*

²*School of Physics, Institute for Research in Fundamental Sciences (IPM), P.O.Box 19395-5531, Tehran, Iran*

³*Department of Physics, Shahid Beheshti University G.C., Evin, Tehran 19839, Iran*

The holographic complexity has been studied in a background which includes a critical point in the dual field theory. We have examined how the complexity rate and the saturation time of dynamical variables in the theory behave as one moves towards the critical point. Two significant results of our analysis are that (i) it takes more time for the complexity in field theory dual to become time dependent as one moves away from the critical point and (ii) near the critical point the complexity starts evolving linearly in time sooner compared to the other points away from it.

Contents

| | |
|--|----|
| I. Introduction and Results | 1 |
| II. The Charged Black Hole Background with Critical Point | 2 |
| III. Complexity | 3 |
| A. Complexity=Action Prescription | 4 |
| B. Numerical Results | 6 |
| Acknowledgement | 9 |
| A. Some details on complexity analytic calculations | 9 |
| References | 10 |

I. INTRODUCTION AND RESULTS

Recently new connections between quantum information and quantum gravity have been developed, attracting a lot of attention in the literature. A promising framework to study these connections is the holographic framework provided by AdS/CFT correspondence [1]. One of these concepts in quantum information theory is the quantum computational complexity. In the holographic context, the quantum complexity is the minimum number of elementary operations (quantum gates) needed to produce a boundary state which is of interest from a fixed reference state. See [2] for the review.

Quantum complexity in AdS/CFT picture sheds light on physics behind the horizon. In fact it was proposed that the quantum information complexity of the boundary field theory state is encoded geometrically in the gravitational dual space-time. A primary example is the eternal two-sided AdS-Schwarzschild black hole which is dual to the thermofield double state in the boundary theory [3]. This is an entangled state of two copies of the boundary conformal field theory. This entanglement is responsible for the geometric connection in the bulk [4]. More specifically it has been shown that the black hole interior grows in time long after the equilibrium is reached [5]. On the other hand one expects that the complexity of the dual thermal plasma to increase long after local equilibrium is reached. In fact the complexity of a state can increase due to its Hamiltonian time evolution and this growth is dual to the late-time growth of the interior. It is conjectured that the complexity continues to grow up to a time scale exponential in the

* hebrahim@ut.ac.ir

† m_asadi@ipm.ir

‡ m_aliakbari@sbu.ac.ir

number of degrees of freedom [6]. Therefore it is proposed that these two descriptions belong to the same phenomena [7].

This proposal has been introduced in two different recipes: to characterize the size of black hole interior with its spatial volume or its action are known as volume [8] or action [9, 10] conjectures in the literature. The complexity equals action includes almost all good features of volume conjecture and in addition one does not need to fix an extra free length scale by hand. Once the length scale is fixed by considering any particular black hole the predictions can be made for the other cases. The action complexity prescription equates the boundary theory complexity with the gravitational action evaluated on a space-time region called Wheeler-de Witt (WdW) patch:

$$\mathcal{C} = \frac{I_{WdW}}{\pi\hbar}. \quad (1)$$

This region is bounded by null surfaces that reach the relevant times on the left and right boundaries. Since holographic complexity has been proposed, a lot of papers have studied different aspects of it [11].

An interesting question that can be asked is about the late-time growth rate of complexity. This proposal asserts that it is proportional to $\frac{2M}{\pi}$ where M is the mass of the black hole. Therefore it is independent of space-time dimension or other information of the boundary theory [9, 10].

In this paper we would like to study the full time evolution of holographic complexity of the charged thermofield double state and its behaviour near the critical point. Therefore we consider a field theory with a critical point whose gravity dual is a charged black hole, discussed in the upcoming section. The field theory is characterized by temperature T and chemical potential μ and its phase diagram contains a first order phase transition line which ends in a critical point. It is characterized by the ratio of $\frac{\mu}{T}$, as expected, since the underlying theory is conformal. Although there are known backgrounds in holographic framework including a critical point in the field theory dual, we choose this background since it can be investigated analytically and one has more control on the calculations [12].

The results of our studies can be summarized as follows. We try to check the possible quantities that are interesting to analyze in this background near the critical point. Firstly the behaviour of the critical time, the time at which the complexity rate becomes non-zero, with respect to $\frac{\mu}{T}$ is studied. The critical time decreases as $\frac{\mu}{T}$ increases and gets its minimum value at the critical point. It means that it takes more time for the complexity in field theory dual to become time dependent as one moves away from the critical point. This behaviour persists for the other time scales in theory such as the saturation time of r_m , the value of r at which the past null rays of WdW patch intersect, and the saturation time of complexity rate. Therefore near the critical point the complexity starts evolving in time linearly sooner compared to the other values of $\frac{\mu}{T}$. We also obtain the dynamical critical exponent using the aforementioned time scales and they all are equal up to less than one percent error.

We have also examined the difference between the saturation time scales of r_m and complexity rate and conclude that this difference reaches zero as one moves towards the critical point. This means that the complexity rate and r_m saturate at the same time at the critical point. For the other values of $\frac{\mu}{T}$ the complexity rate saturates later than r_m .

We also show that the late-time values of r_m monotonically decreases moving towards the critical point in $\frac{\mu}{T}$ parameter space while complexity rate increases at first and as getting closer to the critical point peaks and starts decreasing.

II. THE CHARGED BLACK HOLE BACKGROUND WITH CRITICAL POINT

In this section we review the 5-dim background obtained as a solution to the following gravitational actions action

$$S = \frac{1}{16\pi G_5} \int d^5x \sqrt{-g} \left[R - \frac{f(\phi)}{4} F_{\mu\nu} F^{\mu\nu} - \frac{1}{2} \partial_\mu \phi \partial^\mu \phi - V(\phi) \right], \quad (2)$$

where G_5 is the five dimensional Newton's constant. This action is the gravitational action of 1RCBH model [13] with dilaton potential as

$$V(\phi) = -(8e^{\frac{\phi}{\sqrt{6}}} + 4e^{-\sqrt{\frac{2}{3}}\phi}), \quad (3)$$

and the Maxwell-Dilaton coupling

$$f(\phi) = e^{-2\sqrt{\frac{2}{3}}\phi}. \quad (4)$$

The solution to the equations of motion derived from the action (2) can be summarized as

$$ds^2 = e^{2A(r)}(-h(r)dt^2 + d\vec{x}^2) + \frac{e^{2B(r)}}{h(r)}dr^2, \quad (5)$$

$$\begin{aligned} A(r) &= \ln r + \frac{1}{6}\ln\left(1 + \frac{Q^2}{r^2}\right), \\ B(r) &= -\ln r - \frac{1}{3}\ln\left(1 + \frac{Q^2}{r^2}\right), \\ h(r) &= 1 - \frac{M^2}{r^2(r^2 + Q^2)}, \\ \phi(r) &= -\sqrt{\frac{2}{3}}\ln\left(1 + \frac{Q^2}{r^2}\right), \end{aligned} \quad (6)$$

$$A_t(r) = \left(-\frac{MQ}{r^2 + Q^2} + \frac{MQ}{r_H^2 + Q^2} \right), \quad (7)$$

where A_t is the time component of the gauge field which has been chosen to be zero at the horizon and regular on the boundary. M is the black hole mass and Q is its charge. We set AdS radius equal to one throughout the paper. The boundary of this asymptotically AdS solution is located at $r \rightarrow \infty$ and r_H is the black hole horizon and is obtained from $h(r_H) = 0$,

$$r_H = \sqrt{\frac{\sqrt{Q^4 + 4M^2} - Q^2}{2}}. \quad (8)$$

The chemical potential and the temperature in the dual field theory are

$$\mu = \lim_{r \rightarrow \infty} A_t = \frac{Qr_H}{\sqrt{Q^2 + r_H^2}}, \quad (9)$$

$$T = \frac{\sqrt{-g_{tt}'g_{rr}'}}{4\pi} \Big|_{r=r_H} = \frac{Q^2 + 2r_H^2}{2\pi\sqrt{Q^2 + r_H^2}}. \quad (10)$$

Having obtained $\frac{Q}{r_H}$ in the bulk solution with respect to $\frac{\mu}{T}$ in the boundary we will see that the background considered here contains two different branches of variables $\frac{Q}{r_H}$ corresponding to each value of $\frac{\mu}{T}$. It indicates the existence of a first order phase transition in field theory. The relation between parameters in the bulk and the parameters in field theory dual can be evaluated using (9) and (10)

$$\frac{Q}{r_H} = \sqrt{2} \left(\frac{1 \pm \sqrt{1 - \left(\frac{\sqrt{2}}{\pi} \frac{\mu}{T}\right)^2}}{\frac{\sqrt{2}}{\pi} \frac{\mu}{T}} \right). \quad (11)$$

Using the relations between entropy, s , and charge density, ρ , in terms of the bulk solution parameters Q and r_H one can evaluate the Jacobian $\mathcal{J} = \frac{\partial(s, \rho)}{\partial(T, \mu)}$. If the Jacobian is positive (negative) for the set of parameters in one branch the system is thermodynamically stable (unstable). The two branches intersect at the critical point where $\frac{\mu}{T}^* = \frac{\pi}{\sqrt{2}}$ ($\frac{Q}{r_H} = \sqrt{2}$) and the branch with the parameters satisfying $\frac{Q}{r_H} < \sqrt{2}$ is stable.

Different aspects of this background have been investigated in various papers. For instance in [12] this background has been used as the holographic dual of QCD and the QCD critical point and its exponent has been estimated. Moreover in the dual holographic plasma to this background the bulk viscosity and baryon conductivity have been computed in [14] and consequently the dynamical critical exponent could be obtained. The value of the dynamical critical exponent was also confirmed in [15] and [16] by studying quasi-normal modes and quantum quench in this background, respectively.

III. COMPLEXITY

To describe the quantum complexity of states in the boundary field theory two different holographic procedures have been introduced in the literature. One is complexity equals volume conjecture [8] and the other one action conjecture [9, 10]. In the following we will only concentrate on the action prescription and evaluate it for the background we work on in this paper. The first subsection will be devoted to the analytical results and in the other one we will present the numerical results of this paper.

A. Complexity=Action Prescription

Let's consider a quantum state of a particular time slice of the boundary conformal field theory. The action prescription then relates the complexity of this state to the gravitational action evaluated in the corresponding region in the dual gravity theory called "Wheeler-de Witt" (WdW) patch. This region is enclosed by the future and past null sheets sent from the boundary time slice into the bulk space-time. It is illustrated in figure 1 for the asymptotically AdS eternal black hole background where we have called the boundary time on the left and right boundaries as t_L and t_R . The boundary state we are considering is on the constant time slices denoted by t_L and t_R on the two asymptotic boundaries, $|\psi(t_L, t_R)\rangle$. This thermofield double state is parametrized by mass M , charge Q and chemical potential μ . In fact for the charged background as well as temperature we have the chemical potential to distinguish the boundary states. Please note that we have set $t_L = t_R \equiv \frac{t}{2}$ in this figure. t stands for the boundary time in which we evaluate the time dependence of the complexity.

As shown in figure 1, the time-like killing vectors which correspond to time translation in the background generate upward (downward) flows on the right and left boundaries and hence the action is invariant under shifting the time slices as $t_R + \delta t$ and $t_L - \delta t$. In terms of the boundary theory this corresponds to the invariance of the thermofield double state under an evolution with the Hamiltonian $H_R - H_L$.

To describe the null sheet boundaries of the WdW patch we work with the tortoise coordinate which is defined as

$$dr^* = \frac{e^{B(r)-A(r)}}{h(r)} dr, \quad (12)$$

in our background (5). Integrating the above equation we get

$$r^*(r) = -\frac{\sqrt{2}}{Q^2} \left[\sqrt{\sqrt{Q^4 + 4M^2} - Q^2} \tan^{-1} \sqrt{\frac{r^2 + Q^2}{\sqrt{Q^4 + 4M^2} - Q^2}} - \sqrt{\sqrt{Q^4 + 4M^2} + Q^2} \tan^{-1} \sqrt{\frac{r^2 + Q^2}{\sqrt{Q^4 + 4M^2} + Q^2}} \right]. \quad (13)$$

Then the Eddington-Finkelstein coordinates, u and v are defined as

$$v = \tau + r^*(r), \quad u = \tau - r^*(r), \quad (14)$$

where τ represents the time parametrization of the null sheets which becomes t on the asymptotic boundaries of the background.

The gravitational action that should be calculated here is

$$\begin{aligned} I &= I_{\text{bulk}} + I_{\text{surface}} + I_{\text{joint}} \\ &= \frac{1}{16\pi G_5} \int_M d^5x \sqrt{-g} \left(R - \frac{f(\phi)}{4} F_{\mu\nu} F^{\mu\nu} - \frac{1}{2} \partial_\mu \phi \partial^\mu \phi - V(\phi) \right) \\ &+ \frac{1}{8\pi G_5} \int_{\mathcal{B}} d^4x \sqrt{|h|} K + \frac{1}{8\pi G_5} \int_{\Sigma} d^3x \sqrt{\sigma} \eta \\ &- \frac{1}{8\pi G_5} \int_{\mathcal{B}'} d\lambda d^3\theta \sqrt{\gamma} \kappa + \frac{1}{8\pi G_5} \int_{\Sigma'} d^3x \sqrt{\sigma} a. \end{aligned} \quad (15)$$

The first line is the standard Einstein-Hilbert action in the presence of the cosmological constant $\Lambda = \frac{-6}{L^2}$. The second line contains two terms. The first one is the usual Gibbons-Hawking-York surface term (GHY) for time-like and space-like segments of the boundary which exists on the WdW patch. K in this term is the trace of the extrinsic curvature. The second term gives the contribution from Hayward joint terms which appear in the intersection of the space-like and time-like boundary segments. η is defined as the boost angle between the corresponding normal vectors in the intersection. The last line in the action is added due to the presence of null segments in the WdW patch. The first term is the surface term for the null segments of the boundary and the second term is the joint term corresponding to the intersection of the null segments with the other segments. Please note that we work with the convention in which we choose $\kappa = 0$ following [17, 18]. Also note that there is no intersection between time-like and space-like surfaces in WdW patch and therefore the Hayward joint term in the second line will be zero. After fixing the convention we are ready to calculate each term individually in our charged black hole background. We will give the details in the appendix A and report here the results.

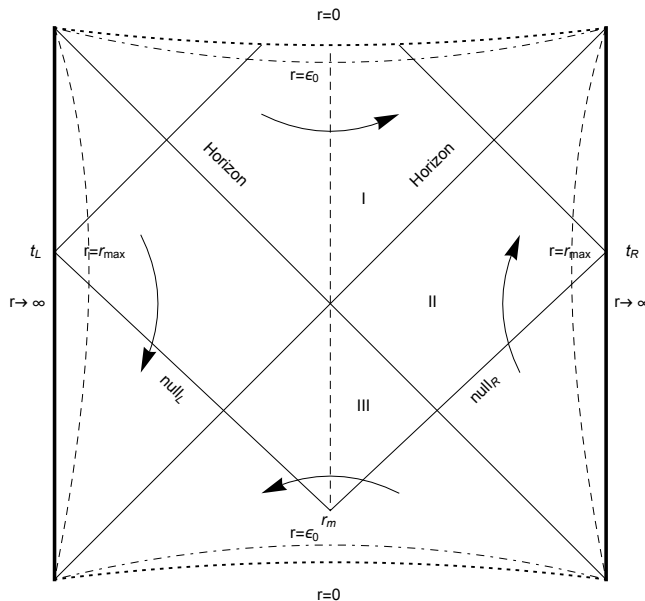


FIG. 1: WdW patch. The arrows present the time directions on each side.

It is important to mention that the complexity can be calculated in two regimes which depend on the position of WdW patch. The first regime for which the complexity is proved to be time independent is where the WdW patch is in contact with the past singularity. Due to time independence of complexity in this regime we will not go through the details of the calculation and refer the interested reader to the papers such as [17], in which this has been done in thorough details.

The second regime is where the past null sheets from the right and left boundaries intersect before crossing the singularity. As we will show later on, and has been shown in related papers such as [17], the complexity is time-dependent in this regime. Therefore we have only plotted the WdW patch which results in the time-dependent part of the complexity of the quantum state in the boundary in figure 1.

One can easily find the time that separates these two regimes which is called critical time t_c , respecting the convention used in the literature. Using the equation of the past null sheets

$$\begin{aligned} \text{null}_L: \quad \tau_L &= -t_L + r_\infty^* - r^*(r), \\ \text{null}_R: \quad \tau_R &= t_R - r_\infty^* + r^*(r), \end{aligned} \quad (16)$$

the critical time is

$$t_c = 2(r_\infty^* - r_0^*), \quad (17)$$

where r_∞^* and r_0^* are calculated at the boundary where $r \rightarrow \infty$ and the singularity at $r \rightarrow 0$, respectively. t_c is the boundary time at which the null sheets from left and right halves of the WdW patch intersect at the past singularity; i.e. $(\tau_L = \tau_R)_{r \rightarrow 0}$. null_L and null_R lines are shown in figure 1.

Having obtained t_c we are in the position to calculate the value of r_m where the two past null sheets from the right and left boundaries intersect before hitting the singularity (as shown in figure 1). Similar to the calculations resulted in (17) using the equations of these null sheets (16) we obtain

$$r^*(r_m) = -\frac{t}{2} + r_\infty^*. \quad (18)$$

It should be emphasized that r_m changes as the boundary time increases and moves towards the horizon in a sufficiently long time. Therefore it is necessary to see how this meeting point r_m evolves with time. Differentiating (18) with respect to time we get

$$\frac{dr_m}{dt} = -\frac{1}{2} h(r) e^{A(r)-B(r)} \Big|_{r=r_m}. \quad (19)$$

This relation suggests that at late times where r_m reaches the horizon, the growth rate of r_m goes to zero as $h(r_H)$ is zero and $e^{A(r)-B(r)}$ reaches a finite value at the horizon. This is confirmed in the next section where we report the numerical results.

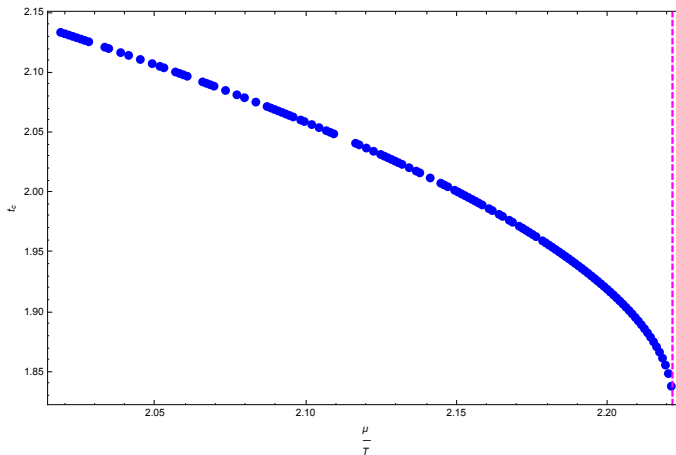


FIG. 2: The behaviour of the critical time t_c with respect to $\frac{\mu}{T}$. The magenta dashed line shows the critical value $\frac{\mu}{T}^*$.

So far we have been trying to obtain some general idea about WdW patch in the background we are interested in. We can start calculating the complexity in the field theory dual to this background using action prescription. As it was mentioned before since we are interested in the time dependence of complexity we only report the calculations and results for the boundary time $t > t_c$. The non-vanishing contributions to the action on WdW patch can be divided into three sets of terms; bulk, GHY and null joint contributions. Due to the symmetry between the left and right halves of the WdW patch, we can calculate the action in the right side of the patch and then multiply it by two. We give the details of the calculations in appendix A and report the time-dependent results here. The complexity in our background becomes

$$\mathcal{C} = \frac{I_{WdW}}{\pi\hbar} = \frac{1}{\pi\hbar}(I_{\text{bulk}} + I_{\text{surf}} + I_{\text{joint}}). \quad (20)$$

Therefore the complexity rate is

$$\begin{aligned} \frac{d\mathcal{C}}{dt} &= \frac{16\pi^2 G_N}{V^{(3)}} \frac{d\mathcal{C}}{dt} \\ &= \int_0^{r_m} e^{4A+B} \left(\frac{2}{3} V(\phi) + \frac{1}{3} f(\phi) e^{-2(A+B)} A_t'^2 \right) dr \\ &\quad + e^{4A(r_m)-B(r_m)} h(r_m) \left[3A'(r_m) \log \left| \frac{h(r_m) e^{2A(r_m)}}{\alpha^2} \right| + \frac{h'(r_m) + 2A'(r_m)h(r_m)}{h(r_m)} \right] + \frac{10}{3} L^2 M^2, \end{aligned} \quad (21)$$

where prime represents the derivative with respect to r . α is a free parameter that has been entered here due to the null joint term, the intersection of null sheets at r_m . It is in fact related to the ambiguity in normalizing the normal vectors to the null sheets, as discussed in [18]. As discussed in [17] we set $\alpha = LT$ where L has already been chosen one in the paper. It should be emphasized here that $\frac{d\mathcal{C}}{dt}$ reduces to eternal AdS black hole result if we initially set $Q \rightarrow 0$ and then send r to zero.

We have presented the analytical results up to here. In the next subsection we will examine these results for different values of the field theory parameters and specifically will see how they behave near the critical point.

B. Numerical Results

In this section we will study the behaviour of the previously obtained results for different values of the parameters relevant to field theory. We are, in particular, interested to see how the field theory quantities behave as we move towards the critical point in the field theory phase space, $\frac{\mu}{T}^*$. Let us first consider the critical time, t_c . Knowing how r^* looks like in terms of the coordinate r , (13), we can obtain how the critical time, (17), evolves as we move nearer to the critical point. This has been plotted in figure 2. Please note that we have set $T = 0.37$ for all the results in this section. A quick conclusion from this figure is that as we move towards the critical point in the parameter $\frac{\mu}{T}$ the critical time decreases and reaches a minimum finite value with an infinite slope. The magenta dashed line shows $\frac{\mu}{T}^*$. Reminding ourselves that the critical time is the time at which the complexity rate becomes non-zero, we can

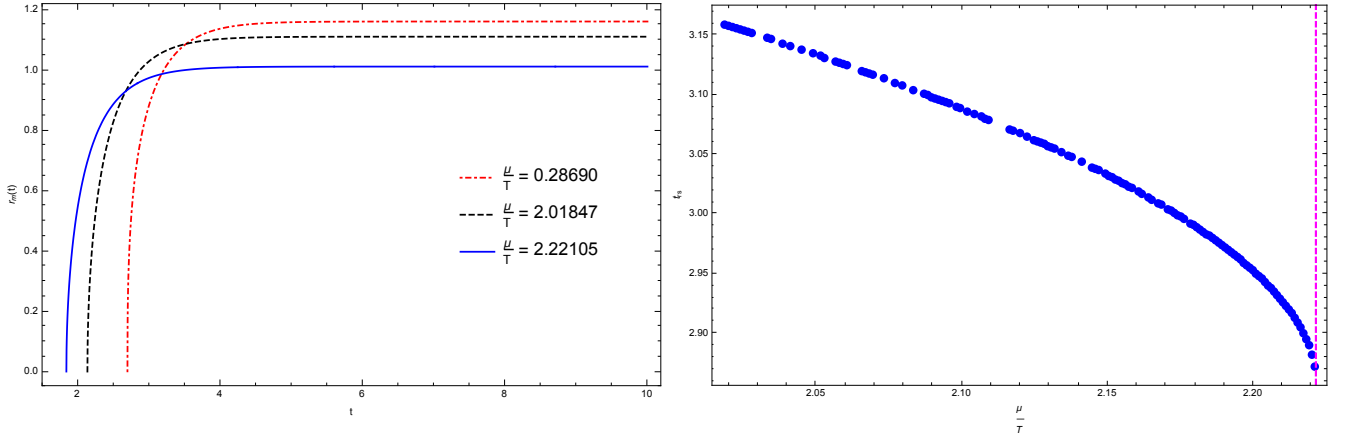


FIG. 3: Left: The behaviour of r_m with respect to time for different values of $\frac{\mu}{T}$. Right: The behaviour of saturation time t_{rs} with respect to $\frac{\mu}{T}$. The magenta dashed line shows the critical value $\frac{\mu}{T}^*$.

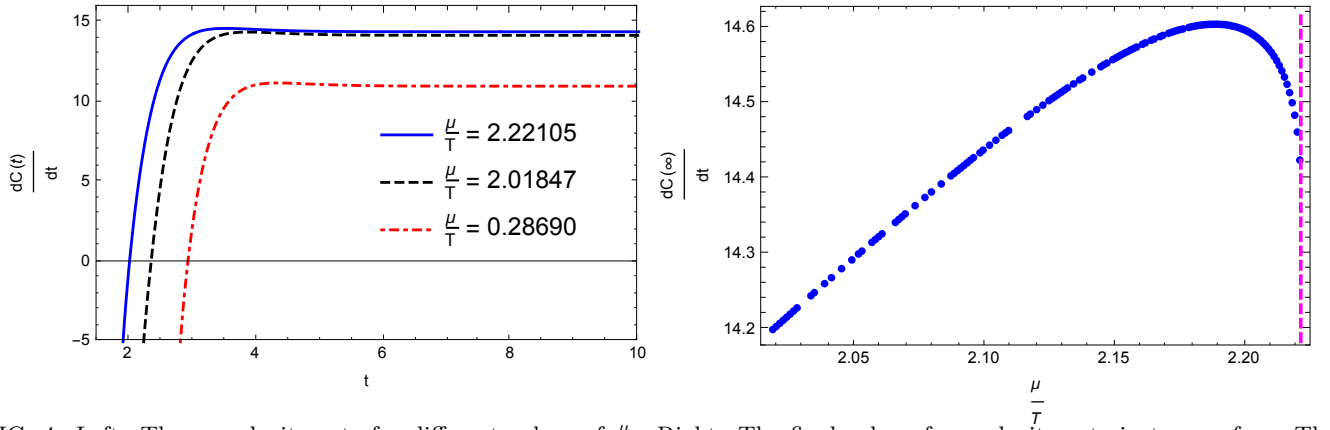


FIG. 4: Left: The complexity rate for different values of $\frac{\mu}{T}$. Right: The final value of complexity rate in terms of m . The magenta dashed line presents $\frac{\mu}{T}^*$.

conclude that the complexity of a thermofield double state produced in field theory starts changing with time sooner as $\frac{\mu}{T}$ moves closer to $\frac{\mu}{T}^*$. Equivalently the complexity of formation of this state in the boundary theory remains constant for longer time as $\frac{\mu}{T}$ decreases.

In figure 3, left panel, we show the result of solving the differential equation (19) numerically by setting the initial condition for $r_m(t_c)$ to be very small such as 0.001 for different values of $\frac{\mu}{T}$. It is obvious that r_m starts from an initial value near the past singularity, at $t = t_c$, and increases until it saturates to a final value which is equal to r_H as it is expected from equation (19). It can be clearly seen in the figure that the final value of r_m decreases for larger $\frac{\mu}{T}$ and therefore we expect that its minimum value occurs at $\frac{\mu}{T}^*$.

An interesting quantity one can study is the r_m saturation time. It's represented as t_{rs} and defined as the time after which the relation $|r_m(\infty) - r_m(t_{rs})| < 0.05 r_m(\infty)$ is always satisfied. It has been plotted in figure 3, right panel, with respect to $\frac{\mu}{T}$. The behaviour is quite similar to figure 2; as we move towards the critical point, r_m saturates and reaches its final value in smaller timescales. Comparing these two figures, one can easily conclude that the smaller t_c gets the smaller t_{rs} is.

The next quantity that its dependence on $\frac{\mu}{T}$ can be studied is the complexity rate in time $\frac{dC}{dt}$. It is plotted in figure 4, left panel. This figure shows that after $t > t_c$ the complexity rate increases up to its maximum value in a short time interval and then relaxes to a constant quantity at late times. As it can be seen in the figure complexity rate reaches the final value from above and similarly to the results reported in the literature the Lloyd's bound, [19], is violated [17]. This constant late-time value depends on Q , M and μ and varies as $\frac{\mu}{T}$ changes. Furthermore, it seems in this plot that as we move towards the critical value of $\frac{\mu}{T}$ the final value of $\frac{dC}{dt}$ increases. We have examined it more closely in figure 4, right panel. $\frac{dC(\infty)}{dt}$ represents the value that the complexity rate relaxes to at late times. The intriguing observation is that the growth of complexity rate at late times peaks slightly before the critical $\frac{\mu}{T}$, magenta dashed line in plot, and then starts decreasing as we get very much closer to the critical point. Therefore two different values of

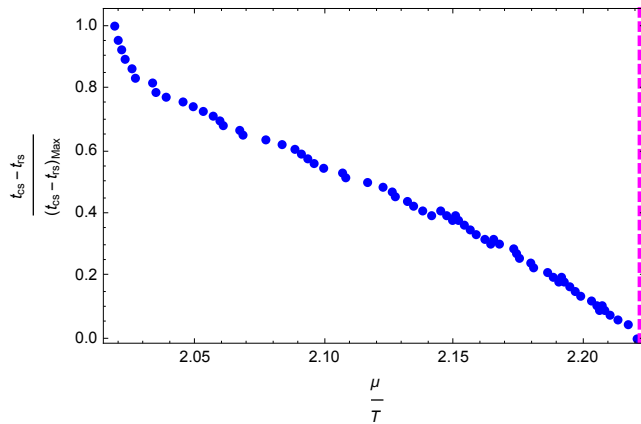


FIG. 5: The numerical difference between the saturation times, $t_{cs} - t_{rs}$ is plotted with respect to $\frac{\mu}{T}$. It can be almost fitted with a linear function.

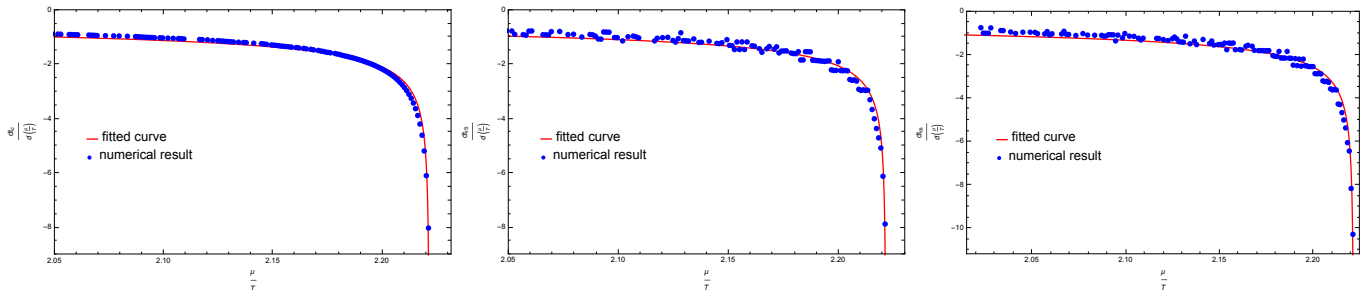


FIG. 6: Left: The slope of the critical time t_c with respect to $\frac{\mu}{T}$. The blue dots are the numerical result and the red curve is the fitted function as $-0.5(\frac{\pi}{\sqrt{2}} - \frac{\mu}{T})^{-0.36762}$. Middle: The slope of the saturation time for r_m , t_{rs} , with respect to $\frac{\mu}{T}$. The fitted curve with the numerical result is $-0.52(\frac{\pi}{\sqrt{2}} - \frac{\mu}{T})^{-0.36242}$. Right: The slope of the saturation time for $\frac{dC}{dt}$, t_{cs} , with respect to $\frac{\mu}{T}$. The fitted curve with the numerical result is $-0.59(\frac{\pi}{\sqrt{2}} - \frac{\mu}{T})^{-0.38065}$.

$\frac{\mu}{T}$ correspond to one specific value of complexity rate. This happens in contrast to the $\frac{\mu}{T}$ dependence of the late-time values of r_m where it continuously decreases moving towards the critical point and reaches its minimum value there. It should also be mentioned that complexity rate in the field theory dual to our background is different from the one dual to usual asymptotically AdS charged black hole backgrounds obtained from Einstein-Maxwell theory in the sense that the presence of non-zero chemical potential does not modify the early time behaviour as we still can see the negative divergent complexity rate there [17].

Another significant result can be obtained if one defines a saturation time for the complexity rate, called t_{cs} , and compare it with the saturation time obtained for the $r_m(t)$ case, t_{rs} , previously. We have defined it numerically similarly to t_{rs} as a time at which the quantity $|\frac{dC(\infty)}{dt} - \frac{dC(t_s)}{dt}| < 0.05 \frac{dC(\infty)}{dt}$ and stays below this limit afterwards. The result for saturation time of complexity rate is similar to t_c and t_{rs} , figures 2 and 3 right, so we have not plotted it here. Moving towards the critical point the saturation time decreases with a seemingly infinite slope. We would also like to examine if the relaxation of r_m and complexity rate to their late-time values happen at the same time. The result has been plotted in figure 5 where the numerical difference, $t_{cs} - t_{rs}$ has been scaled with its maximum value in the plot. The first observation is that this quantity decreases by raising $\frac{\mu}{T}$ almost linearly. It's also illuminating to see that as one moves towards the critical point, magenta dashed line in plot, this difference becomes less and less significant until it gets an infinitesimally small value which is almost zero. Therefore r_m and $\frac{dC}{dt}$ happens at almost the same time very close to the critical point, $\frac{\mu}{T}^*$.

As it was mentioned in the previous paragraph, looking closely at the figures 2, 3 right and the one for t_{cs} which we have not plotted here, the behaviour of t_c , t_{rs} and t_{cs} near the critical point are the same. They all decrease as moving towards the critical point and reach a finite value there but the slope of the change in time with respect to $\frac{\mu}{T}$ seems to go to infinity. It's intriguing to check how the slope changes as a function of $(\frac{\mu}{T}^* - \frac{\mu}{T})$. One can assume that if the slope function fits with $(\frac{\mu}{T}^* - \frac{\mu}{T})^{-\theta}$ the value of θ gives the dynamical critical exponent in the field theory dual to this background. The dynamical critical exponent obtained using the conserved currents in the field theory dual is

0.5 [14]. In fact this has been checked and confirmed in the papers [15] and [16] where the authors have studied the quasi normal modes and equilibration time behaviour near the critical point, respectively.

The slope near the critical point has been evaluated using

$$\frac{dJ}{d\frac{\mu}{T}}(i) = \frac{J(i+1) - J(i)}{\frac{\mu}{T}(i+1) - \frac{\mu}{T}(i)}, \quad (22)$$

where J is t_c , t_{rs} or t_{cs} . The results have been plotted in figure 6. The blue points show the numerical result and the red curve is the fitted function $(\frac{\mu}{T}^* - \frac{\mu}{T})^{-\theta}$ where we have used the "find fit" command in mathematica. The result for θ is 0.36242, 0.367616 and 0.38065 for plots left, middle and right in figure 6, respectively. This is a very interesting result as, although we have calculated θ from three basically different quantities but their values are very close and no matter how accurate we calculate it still they remain almost equal. We should point out that depending on how many data points we consider the value of θ can vary between 0.3 and 0.5. The important result we insist on here is that considering a specific number of data points the critical exponent obtained from these three function t_c , t_{rs} and t_{cs} remain almost the same. One of these quantities was critical time that is the time at which the complexity becomes time dependent and the other one is the saturation time at which r_m relaxes to its final value which is r_H , the horizon radius of the background. It is interesting, as we will try afterwards, to see if the other quantities calculated in this background behave similarly near the critical point.

Acknowledgement

We would like to thank M. M. Sheikh-Jabbari, M. R. Mohammadi Mozafar, R. Fareghbal and M. Lezgi for fruitful discussions and comments. M. A. would like to thank School of Physics of Institute for research in fundamental sciences (IPM) for the research facilities and environment.

Appendix A: Some details on complexity analytic calculations

As it was discussed in III the complexity in its action prescription can be evaluated by calculating the action (15) on WdW patch in figure 1. The time-dependent part of the complexity is the one that is important for us since it results in complexity rate. We will give some details on how to calculate it in the following:

• Bulk Contribution

It was mentioned previously that the first line in the gravitational action (15) gives the bulk contribution. The curvature R in the background we consider here is $-\frac{d(d+1)}{L^2} = -\frac{20}{L^2}$. Therefore we have

$$\begin{aligned} I_{\text{bulk}} &= \frac{V^{(3)}}{16\pi G_N} \int d\tau dr \sqrt{-g} \left(R - \frac{f(\phi)}{4} F_{\mu\nu} F^{\mu\nu} - \frac{1}{2} \partial_\mu \phi \partial^\mu \phi - V(\phi) \right) \\ &= \frac{V^{(3)}}{16\pi G_N} \int d\tau dr \left(-\frac{16r^3}{L^5} - \frac{8r^3}{3L^5} \left(\frac{r^2 + Q^2}{r^2} \right) + \frac{4M^2 Q^2}{3L^3 r^3} \left(\frac{r^2 + Q^2}{r^2} \right)^{-2} \right) \end{aligned} \quad (A1)$$

$$= \frac{V^{(3)}}{16\pi G_N} \int d\tau dr \mathcal{I}(r) \quad (A2)$$

where $V^{(3)}$ is the volume of the spatial geometry. Due to the symmetry between left and right sides of WdW patch we can evaluate this integral on the right side and then multiply it by two. We will repeat this in the other calculations too. Different parts of this patch, as denoted by I, II and III in figure 1, produce

$$I_{\text{bulk}}^I = \frac{2V^{(3)}}{16\pi G_N} \int_0^{r_h} dr \mathcal{I}(r) \int_0^{t_R + r_\infty^* - r^*(r)} d\tau = \frac{V^{(3)}}{8\pi G_N} \int_0^{r_h} dr \mathcal{I}(r) (t_R + r_\infty^* - r^*(r)), \quad (A3)$$

$$I_{\text{bulk}}^{II} = \frac{2V^{(3)}}{16\pi G_N} \int_{r_h}^{r_{\text{max}}} dr \mathcal{I}(r) \int_{t_R - r_\infty^* + r^*(r)}^{t_R + r_\infty^* - r^*(r)} d\tau = \frac{V^{(3)}}{4\pi G_N} \int_{r_h}^{r_{\text{max}}} dr \mathcal{I}(r) (r_\infty^* - r^*(r)), \quad (A4)$$

$$I_{\text{bulk}}^{III} = \frac{2V^{(3)}}{16\pi G_N} \int_{r_m}^{r_h} dr \mathcal{I}(r) \int_{t_R - r_\infty^* + r^*(r)}^0 d\tau = \frac{V^{(3)}}{8\pi G_N} \int_{r_m}^{r_h} dr \mathcal{I}(r) (-t_R + r_\infty^* - r^*(r)). \quad (A5)$$

As it can be seen the contribution of the part II in the action is time independent. Since we have assumed $t_R = t_L = \frac{t}{2}$ and using the left-right symmetry the total contribution of the bulk action becomes

$$\frac{dI_{\text{bulk}}}{dt} = \frac{V^{(3)}}{16\pi G_N} \int_0^{r_m} \mathcal{I}(r) dr, \quad (\text{A6})$$

where $I_{\text{bulk}} = I_{\text{bulk}}^I + I_{\text{bulk}}^{II} + I_{\text{bulk}}^{III}$.

• GHY Surface Term

As mentioned in section III GHY terms are only defined on time-like or space-like surfaces. Since we are only interested in time-dependent contributions to the action the only non-zero contributions come from future singularity and the uv cut-off in asymptotic boundaries. In order to calculate the GHY part of the action we need to have the trace of the extrinsic curvature on these two r constant surfaces. It is defined as $K = h^{ab}K_{ab} = \nabla_a n^a$ where h_{ab} is the induced metric and n_a is the normal vectors for these surfaces. Note that we use a and b letters for the coordinates on the time-like or space-like surfaces. In general for any $r = \text{constant}$ surface which is defined as $\Phi(r) = r - \text{constant}$ we have

$$n_r = \frac{\varepsilon}{\sqrt{|g^{rr}\partial_r\Phi\partial_r\Phi|}} \Big|_{r=\text{constant}}, \quad (\text{A7})$$

where $\varepsilon = +1, -1$ for time-like and space-like surfaces, respectively. Therefore the final result for GHY action becomes

$$\begin{aligned} I_{\text{surf}}^{\text{future}} &= \frac{V^{(3)}}{8\pi G_N} h(r) e^{4A(r)-B(r)} \left(8A'(r) + \frac{h'(r)}{h(r)} \right) \int_0^{t_R+r_\infty^*-r^*(r)} d\tau \Big|_{r=\epsilon_0}, \\ I_{\text{surf}}^{\text{uv}} &= \frac{V^{(3)}}{8\pi G_N} h(r) e^{4A(r)-B(r)} \left(8A'(r) + \frac{h'(r)}{h(r)} \right) \int_{t_R-r_\infty^*+r^*(r)}^{t_R+r_\infty^*-r^*(r)} d\tau \Big|_{r=r_{\text{max}}}, \end{aligned} \quad (\text{A8})$$

and we define $I_{\text{surf}} = I_{\text{surf}}^{\text{future}} + I_{\text{surf}}^{\text{uv}}$.

• Null Joint Contribution

Normal vectors to the past null boundaries are

$$(K_L^{(\alpha)})_\mu = \left(-\alpha, \alpha \frac{e^{B-A}}{h}\right), \quad (K_R^{(\alpha)})_\mu = \left(\alpha, \alpha \frac{e^{B-A}}{h}\right), \quad (\text{A9})$$

where α is the normalization constant which should be fixed (Discussion on ambiguities regarding the null segments can be found in [18]). The joint action is defined as

$$I_{\text{joint}} = \frac{1}{8\pi G_N} \int d^3x \sqrt{\sigma} \log \left| \frac{1}{2} K_L \cdot K_R \right|. \quad (\text{A10})$$

Therefore we have

$$\begin{aligned} I_{\text{joint}} &= -\frac{V^{(3)}}{8\pi G_N} \left[e^{3A(r)} \log \left| \frac{h(r) e^{2A(r)}}{\alpha^2} \right| \right] \Big|_{r=r_m}, \\ \frac{dI_{\text{joint}}}{dt} &= \frac{V^{(3)}}{16\pi G_N} \left\{ e^{4A(r)-B(r)} h(r) \left(3A'(r) \log \left| \frac{h(r) e^{2A(r)}}{\alpha^2} \right| + \frac{h'(r) + 2A'(r)h(r)}{h(r)} \right) \right\} \Big|_{r=r_m}. \end{aligned} \quad (\text{A11})$$

• Total Action

The rate of growth of holographic complexity is given by

$$\frac{d\mathcal{C}}{dt} = \frac{1}{\pi} \frac{d}{dt} (I_{\text{bulk}} + I_{\text{joint}} + I_{\text{surf}}). \quad (\text{A12})$$

[1] J. M. Maldacena, ‘‘The Large N limit of superconformal field theories and supergravity,’’ Int. J. Theor. Phys. **38**, 1113 (1999) [Adv. Theor. Math. Phys. **2**, 231 (1998)] [hep-th/9711200].

- [2] S. Aaronson, “The Complexity of Quantum States and Transformations: From Quantum Money to Black Holes,” arXiv:1607.05256 [quant-ph].
- [3] J. M. Maldacena, “Eternal black holes in anti-de Sitter,” JHEP **0304**, 021 (2003) [hep-th/0106112].
- [4] J. Maldacena and L. Susskind, “Cool horizons for entangled black holes,” Fortsch. Phys. **61**, 781 (2013) [arXiv:1306.0533 [hep-th]].
- [5] T. Hartman and J. Maldacena, “Time Evolution of Entanglement Entropy from Black Hole Interiors,” JHEP **1305**, 014 (2013) [arXiv:1303.1080 [hep-th]].
- [6] A. R. Brown and L. Susskind, “Second law of quantum complexity,” Phys. Rev. D **97**, no. 8, 086015 (2018) [arXiv:1701.01107 [hep-th]].
- [7] L. Susskind, “Computational Complexity and Black Hole Horizons,” [Fortsch. Phys. **64**, 24 (2016)] Addendum: Fortsch. Phys. **64**, 44 (2016) [arXiv:1403.5695 [hep-th], arXiv:1402.5674 [hep-th]].
- [8] D. Stanford and L. Susskind, “Complexity and Shock Wave Geometries,” Phys. Rev. D **90**, no. 12, 126007 (2014) [arXiv:1406.2678 [hep-th]].
- [9] A. R. Brown, D. A. Roberts, L. Susskind, B. Swingle and Y. Zhao, “Holographic Complexity Equals Bulk Action?,” Phys. Rev. Lett. **116**, no. 19, 191301 (2016) [arXiv:1509.07876 [hep-th]].
- [10] A. R. Brown, D. A. Roberts, L. Susskind, B. Swingle and Y. Zhao, “Complexity, action, and black holes,” Phys. Rev. D **93**, no. 8, 086006 (2016) [arXiv:1512.04993 [hep-th]].
- [11] S. Chapman, H. Marrochio and R. C. Myers, “Complexity of Formation in Holography,” JHEP **1701**, 062 (2017) doi:10.1007/JHEP01(2017)062 [arXiv:1610.08063 [hep-th]]; R. Jefferson and R. C. Myers, “Circuit complexity in quantum field theory,” JHEP **1710**, 107 (2017) doi:10.1007/JHEP10(2017)107 [arXiv:1707.08570 [hep-th]]; S. Bolognesi, E. Rabinovici and S. R. Roy, “On Some Universal Features of the Holographic Quantum Complexity of Bulk Singularities,” JHEP **1806**, 016 (2018) doi:10.1007/JHEP06(2018)016 [arXiv:1802.02045 [hep-th]]; R. Abt, J. Erdmenger, H. Hinrichsen, C. M. Melby-Thompson, R. Meyer, C. Northe and I. A. Reyes, “Topological Complexity in AdS₃/CFT₂,” Fortsch. Phys. **66**, no. 6, 1800034 (2018) doi:10.1002/prop.201800034 [arXiv:1710.01327 [hep-th]]; S. Chapman, M. P. Heller, H. Marrochio and F. Pastawski, “Toward a Definition of Complexity for Quantum Field Theory States,” Phys. Rev. Lett. **120**, no. 12, 121602 (2018) doi:10.1103/PhysRevLett.120.121602 [arXiv:1707.08582 [hep-th]]; C. A. Agn, M. Headrick and B. Swingle, “Subsystem Complexity and Holography,” arXiv:1804.01561 [hep-th]; M. Alishahiha, K. Babaei Velni and M. R. Mohammadi Mozaffar, “Subregion Action and Complexity,” arXiv:1809.06031 [hep-th]; M. Alishahiha, A. Faraji Astaneh, M. R. Mohammadi Mozaffar and A. Mollabashi, “Complexity Growth with Lifshitz Scaling and Hyperscaling Violation,” JHEP **1807**, 042 (2018) doi:10.1007/JHEP07(2018)042 [arXiv:1802.06740 [hep-th]]; S. A. Hosseini Mansoori, V. Jahnke, M. M. Qaemmaqami and Y. D. Olivas, “Holographic complexity of anisotropic black branes,” arXiv:1808.00067 [hep-th]; A. Reynolds and S. F. Ross, “Divergences in Holographic Complexity,” Class. Quant. Grav. **34**, no. 10, 105004 (2017) doi:10.1088/1361-6382/aa6925 [arXiv:1612.05439 [hep-th]]; Y. Zhao, “Complexity and Boost Symmetry,” Phys. Rev. D **98**, no. 8, 086011 (2018) doi:10.1103/PhysRevD.98.086011 [arXiv:1702.03957 [hep-th]].
- [12] O. DeWolfe, S. S. Gubser and C. Rosen, “A holographic critical point,” Phys. Rev. D **83**, 086005 (2011) [arXiv:1012.1864 [hep-th]].
- [13] S. S. Gubser, “Thermodynamics of spinning D3-branes,” Nucl. Phys. B **551**, 667 (1999) doi:10.1016/S0550-3213(99)00194-7 [hep-th/9810225]; K. Behrndt, M. Cvetič and W. A. Sabra, “Nonextreme black holes of five-dimensional N=2 AdS supergravity,” Nucl. Phys. B **553**, 317 (1999) doi:10.1016/S0550-3213(99)00243-6 [hep-th/9810227]; P. Kraus, F. Larsen and S. P. Trivedi, “The Coulomb branch of gauge theory from rotating branes,” JHEP **9903**, 003 (1999) doi:10.1088/1126-6708/1999/03/003 [hep-th/9811120]; R. G. Cai and K. S. Soh, “Critical behavior in the rotating D-branes,” Mod. Phys. Lett. A **14**, 1895 (1999) doi:10.1142/S0217732399001966 [hep-th/9812121]; M. Cvetič and S. S. Gubser, “Phases of R charged black holes, spinning branes and strongly coupled gauge theories,” JHEP **9904**, 024 (1999) doi:10.1088/1126-6708/1999/04/024 [hep-th/9902195]; M. Cvetič and S. S. Gubser, “Thermodynamic stability and phases of general spinning branes,” JHEP **9907**, 010 (1999) doi:10.1088/1126-6708/1999/07/010 [hep-th/9903132].
- [14] O. DeWolfe, S. S. Gubser and C. Rosen, “Dynamic critical phenomena at a holographic critical point,” Phys. Rev. D **84**, 126014 (2011) [arXiv:1108.2029 [hep-th]].
- [15] S. I. Finazzo, R. Rougemont, M. Zaniboni, R. Critelli and J. Noronha, “Critical behavior of non-hydrodynamic quasinormal modes in a strongly coupled plasma,” JHEP **1701**, 137 (2017) [arXiv:1610.01519 [hep-th]].
- [16] H. Ebrahim and M. Ali-Akbari, “Dynamically probing strongly-coupled field theories with critical point,” Phys. Lett. B **783**, 43 (2018) [arXiv:1712.08777 [hep-th]].
- [17] D. Carmi, S. Chapman, H. Marrochio, R. C. Myers and S. Sugishita, “On the Time Dependence of Holographic Complexity,” JHEP **1711**, 188 (2017) [arXiv:1709.10184 [hep-th]].
- [18] L. Lehner, R. C. Myers, E. Poisson and R. D. Sorkin, “Gravitational action with null boundaries,” Phys. Rev. D **94**, no. 8, 084046 (2016) [arXiv:1609.00207 [hep-th]].
- [19] S. Lloyd, “Ultimate physical limits to computation,” Nature **406** (2000), no. 6799 10471054 quant-ph/9908043.